ORIGINAL PAPER

CHARACTERIZATION OF A GRECO-ROMAN STUCCO MASK (REG. NO. 229) PRESERVED AT THE NATIONAL MUSEUM OF EGYPTIAN CIVILIZATION, CAIRO, EGYPT

ABDULLAH M.A. KAMEL[1,*], MONA F. ALI[1], MOHAMMED S.A. KHEDR[2], HUSSEIN H. MAREY MAHMOUD[1]

Manuscript received: 22.09.2022; Accepted paper: 18.08.2023; Published online: 30.09.2023.

Abstract. *The Greco-Roman stucco masks are of great historical, artistic and religious importance. According to the restoration-conservation strategies, the detailed mineral characterization of artifacts is an important step that facilitates the selection of appropriate restoration procedures. Different characterization techniques such as USB digital microscope, scanning electron microscopy–energy dispersive X-ray analysis, X-ray diffraction analysis (XRD), thermal analysis (DTA/DTG), Fourier transform infrared and micro-Raman spectroscopies were used. The results indicated that gypsum is the main component of the stucco mask. As well, calcite was found as an impurity or an addition together with halite and anhydrite as deterioration products. The iron nail corrosion was the reason for a notable discoloration to the stucco mask. FTIR analysis confirms that animal glue is the adhesive material used for the reassembly of the mask. The used pigments for painting the mask are hematite for red-orange color, mixture of hematite and magnetite for brown color and mixture of gypsum and hematite for the white brown color.*

Keywords: *Greco-Roman; stucco mask; gypsum; pigments; analysis.*

1. INTRODUCTION

Stucco masks were used as funerary mummy decorations by covering the face, the head and the chest. These objects were influenced strongly by the ancient Egyptian religious traditions in terms of decoration and their purpose of use [1]. The ancient Egyptians believed in resurrection and immortality after death, and these stucco masks were used to achieve that belief [2]. These funerary masks were found in Egypt from the First Dynasty to the first century AD [3]. Actually, the application of three dimensional stucco masks started a while earlier when Aïn Ghazal stucco statues from the 7th Millennium BC were discovered in Jordan [4].

Worthy to state that covering the face by a stucco mask was not used only to physically and magically protect it and substitute the mummified head while loss; it was used to elevate the deceased from a human to a divine status. Really, the mass production of these masks prevented their facial features from being naturalistic, but this did not diminish their religious job or the magical power linked to them [5].

The heads of masks were cast mainly in previously prepared moulds, then the fine details; such as coiffure, dimples, cut of beard or any protruding parts were executed later through modeling and/or incision. Finally, the selected pigments were applied by painting

[1] Cairo University, Faculty of Archaeology, Conservation Department, 12613 Giza, Egypt.
[*] *Corresponding author: dandarawy_241@cu.edu.eg.*
[2] National Museum of Egyptian Civilization, Ministry of Tourism and Antiquities, Cairo, Egypt.

technique. Examination and analysis of stucco masks provide valuable information about their implementation techniques and their mineralogical composition. Therefore, these scientific tools are important to discover the archaeological and technical values associated with such objects. Besides, studying the deterioration factors and aspects allows developing a suitable strategy for their restoration and conservation [6, 7].

The principal aim of this study was to characterize a Greco-Roman stucco mask from the excavations of the American University in Cairo (AUC), preserved at the National Museum of Egyptian Civilization (NMEC) (Reg. No. 229, Fig. 1) by examination and analysis of the stucco body materials, pigments and the main deterioration aspects.

2. MATERIALS AND METHODS

2.1. SAMPLING

Representative samples were collected carefully from deteriorated, separated and invisible parts from the studied stucco mask (the stucco material, pictorial layer and areas of previous restorations) to identify their mineralogical composition and deterioration aspects. Table 1 illustrates the description of the studied samples and the applied analytical methods for each sample (note: sometimes the same sample was analyzed by many methods, such as the case of samples 1A, 1C, 1D and 1E).

Table 1. Description of the studied samples from the mask and the used analytical methods.

Code	Sample description	Method of examination/analysis
1A	Intact stucco sample	USB, XRD
1C	Intact stucco sample	SEM- EDX
1D	Intact stucco sample	FTIR
1E	Intact stucco sample	DTA-DTG
2A	Intact stucco sample	USB, XRD
3	The used material in adhesion and reassembly of the mask	USB, FTIR
6B	Black pigment from chest decoration	USB
4R	Red pigment from chest edges	USB, Raman analysis
5B	Brown pigment from chest	USB, Raman analysis
7WB	White-Brown pigment from the face	USB, Raman analysis
8C	Stained stucco sample with iron nails corrosion	USB, XRD

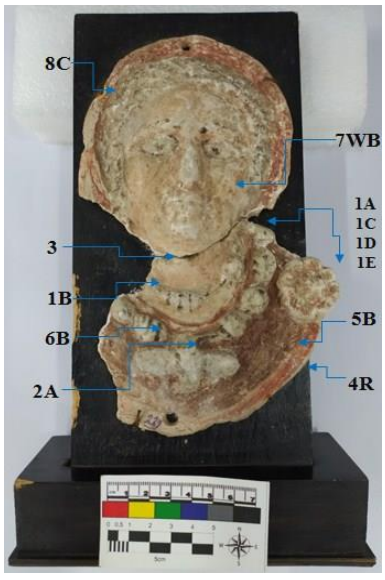

Figure 1. The studied stucco mask and locations of collected samples.

2.2. EXAMINATION BY USB DIGITAL MICROSCOPE

The microscopic features of surfaces of samples from the studied stucco mask were examined using a handheld USB digital microscope (model PZ01, made by Shenzhen Supereyes Co. Ltd, China) with the following technical specification: image sensor 0.3 Mega pixels, magnification factor 10~500 times, photo capture resolution 640×480,320×240 and LED illumination light resource adjustable by a control wheel.

2.3. X-RAY DIFFRACTION ANALYSIS

The X-ray diffraction patterns of three stucco samples were obtained using a Philips PW3710/31 diffractometer at 40 kV and 30 mA. The measurements were made at room temperature. The reference database used for matching is PDF4. Preparation of each sample consisted of grinding the dry sample on one direction, by using a mortar and pestle to obtain a fine powder, which then will be mounted in the sample holder of the diffractometer.

2.4. SCANNING ELECTRON MICROSCOPY- ENERGY DISPERSIVE X-RAY ANALYSIS

The morphology of the stucco mask samples and their chemical composition were recorded by a scanning electron microscope attached with Energy Dispersive X-ray (EDX) Unit: Model Quanta 250 Field Emission Gun (FEG)-FEI Company, Netherlands, with an accelerating voltage 20 kV, magnification 14x up to 1000000 and resolution for Gun.1n), without coating the samples with a highly conductive thin film of gold. The Scanning Electron Microscopy (SEM-EDX) analysis was done at the National Research Center labs, Giza, Egypt.

2.5. FTIR ANALYSIS

A group of FTIR spectra was recorded on the stucco and the used material in adhesion and reassembly of the mask by a Nicolet 760 FTIR spectrometer, in the frequency range of 4000-400 cm^{-1}, with resolution of 4 cm^{-1}, at the micro analytical center of Cairo University, Egypt.

2.6. DTA/DTG ANALYSIS

Differential thermal analysis (DTA) and Thermo gravimetric analysis (TGA) on the stucco sample of the mask were done by (Shimadzu, DTG 60, Japan), using a rate temperature of 10 ^{o}C/min, hold temperature =1000 ^{o}C, atmosphere: nitrogen rate flow 20/min.

2.7. MICRO-RAMAN SPECTROSCOPY

Three pigment grains with red, brown, and white brown color hues were studied by a Renishaw HORIBA spectrometer (which was operated with a laser excitation line of 532 nm)

coupled with 'OPUS software'. The spectrometer comes with an Olympus BX microscope which facilities the analysis of particles in a deep inner matrix with a 2 µm resolution. The analysis was performed at Faculty of Nanotechnology for Postgradates of Cairo University.

3. RESULTS AND DISCUSSIONS

3.1. MICROSCOPIC EXAMINATION

The observations made by the USB digital microscope on the studied samples revealed the following results which are resumed in Fig. 2 and Table 2.

Table 2. The USB digital microscope examination results of the studied stucco mask samples.

Figure	USB digital microscopic observations on the studied stucco mask samples.
Fig. 2-1A	Noticeable glossiness probably due to old treatments of the stucco surface.
Fig. 2-2A	An erosion in the surface of the stucco layer, which showed its implementation from more than one layer, as well; fine sand grains in the stucco were also observed.
Fig. 2-3	It shows the adhesive material that was used to reassemble the stucco mask, in addition to the appearance of some fibers, which may be due to the cotton used in previous conservation procedures.
Fig. 2-4R	It shows the red pigment used on the chest, and some missing parts.
Fig. 2-5B	It shows the brown pigment used on the chest with some missing parts.
Fig. 2-6B	It shows the black pigment used for chest decoration, some parts of which have been lost because of the deterioration of stucco layer.
Fig. 2-7WB	It shows the white-brown pigment from the face which used to give the skin color.
Fig. 2-8C	It shows the corrosion of iron nail which caused the staining of the surrounding stucco material by the corrosion products.
Fig. 2-OR	Fiber traces confirm the old conservation procedures which applied to the chest surface of the mask.

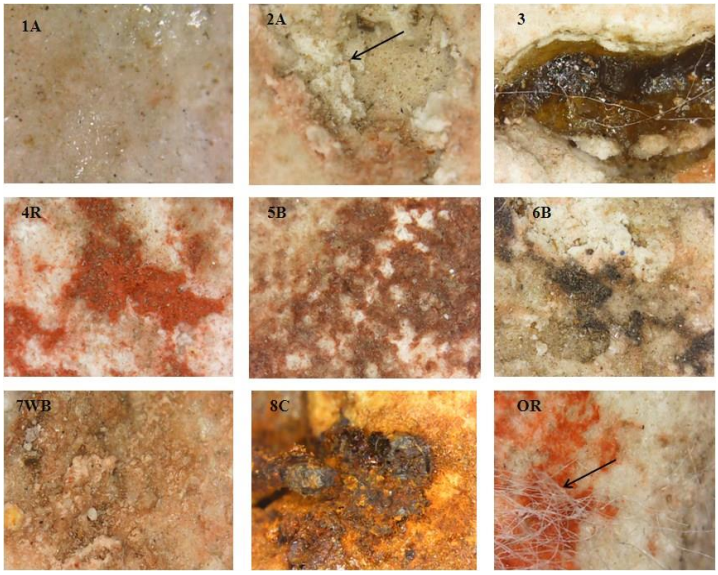

Figure 2. The USB digital microscope examination results of the studied stucco mask.

3.2. X-RAY DIFFRACTION ANALYSIS

The XRPD patterns of the studied stucco samples from the stucco mask No. 229 (Figs. 3 and 4) indicate the following results: The semi-quantitative analysis of the mineralogical components of samples (1A and 2A) indicates gypsum ($CaSO_4 \cdot 2H_2O$, 62% wt.) as the main component of the stucco mask. The ratio of calcite ($CaCO_3$, 10.7% wt.) may be resulted from an addition of limestone powder [8], which occurred as traces in the gypsum raw materials

before calcinations [9]. More, it is probably resulted from mixing of slaked lime through preparation of the stucco mix to improve the characteristics of the produced stucco [10].

- The detection of anhydrite ($CaSO_4$, 9.4% wt.) is highly resulted from the exposure to high temperature and relative humidity for a long time or from an impurity in the gypsum raw materials and not affected by the calcination process. Furthermore, it is acceptable that it may be resulted from the overheating of gypsum raw materials [11-13].

- The detection of halite salt (NaCl), especially in sample 2A, is most probably related to the burial environment of the stucco mask or the uncontrolled storage conditions [14].

- The traces of bassanite ($CaSO_4 \cdot 0.5H_2O$) are indications for the active transformation from gypsum to anhydrite [15].

- The low ratio of quartz (SiO_2) in the samples proves that it occur an impurity in the raw materials and it was not an intentional addition to the stucco mix.

- The detection of iron corrosion products (limonite $FeO(OH) \cdot nH_2O$, goethite α-FeOOH and hematite α-Fe_2O_3) proves the effect of iron nail corrosion which caused the staining of the surrounding stucco material (Fig. 4) [16].

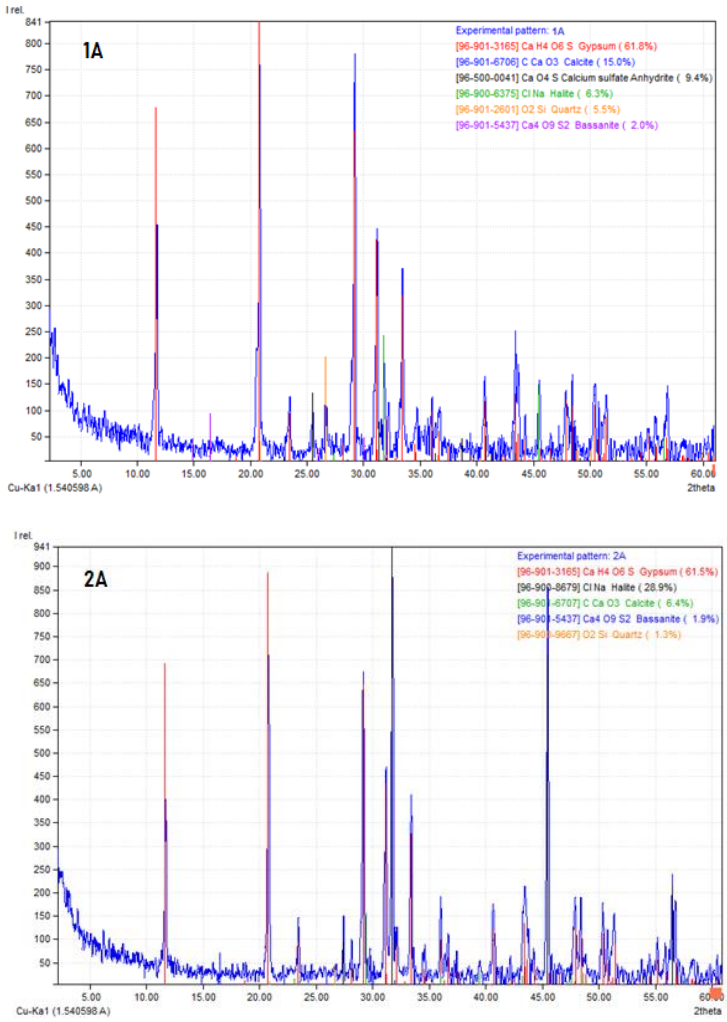

Figure 3. X-ray diffraction patterns of the studied stucco mask No. 229 (samples 1A & 2A) indicate that gypsum is the main component of the stucco mask together with ratios of calcite, quartz. While the detection of halite, anhydrite and bassanite is related to deterioration aspects.

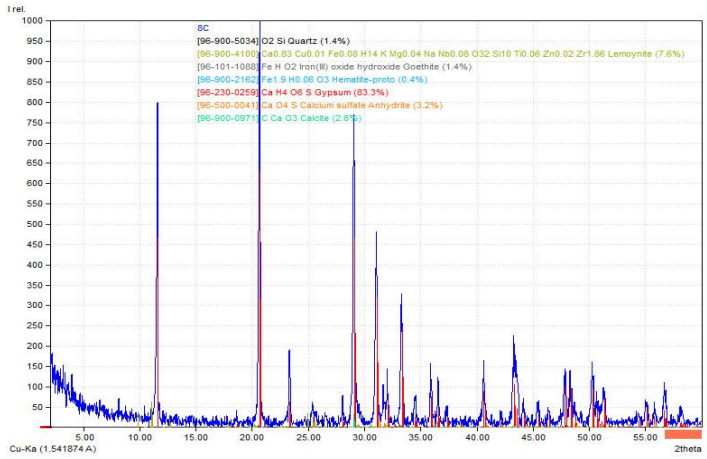

Figure 4. X-ray diffraction pattern of the stucco mask stained with iron nails corrosion (sample 8C).

3.3. SCANNING ELECTRON MICROSCOPY-ENERGY DISPERSIVE X-RAY ANALYSIS

The results of EDX analysis of sample (1C) (Fig. 5) proved the presence of the following elements: calcium (Ca), sulfur (S) carbon (C), oxygen (O), silicon (Si), which may give an evidence to the occurrence of gypsum phases, calcite and quartz [17]. These results are compatible with the previously given XRD results.

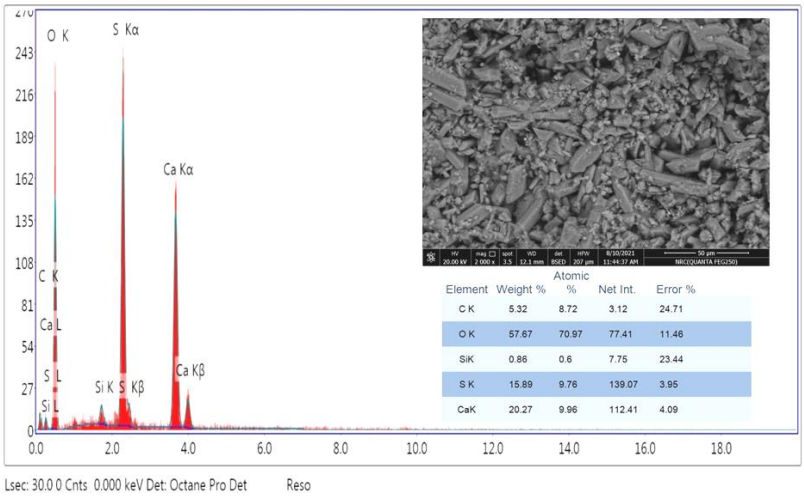

Figure 5. EDX spectrum and SEM image of stucco sample from the stucco mask, the detected elements confirm the results of XRD analysis. While the needle like and elongated crystals in the scanning electron micrograph confirm that gypsum is the main component of the used stucco.

3.4. FTIR ANALYSIS

By comparing the functional groups of animal glue standard samples with the results of sample (3) of the used material in the adhesion and the reassembly of the mask, it became obvious that animal glue had been used to reassemble the studied mask. Also, comparing the functional groups of sample (1D) of the intact stucco sample proves that the stucco sample consists mainly of gypsum as a binding material [18-20] (Table 3 and Fig. 6).

Table 3. The FTIR functional groups of samples 1D and 3.

Functional group bands	Wave numbers (cm^{-1})
Sample 3 (animal glue sample)	
N-H stretching band	3405 cm^{-1}
C-H stretching band	2920 cm^{-1} : 2852 cm^{-1}
C=O stretching band	1623 cm^{-1}
C-N–H bending band	1556 cm^{-1}
C-H bending band	1454 cm^{-1}
Sample 1D (the intact stucco sample)	
Asymmetric SO_4^{2-} stretching band	1120 cm^{-1}
Antisymmetric and symmetric O-H stretching band	3546 cm^{-1} : 3406 cm^{-1}

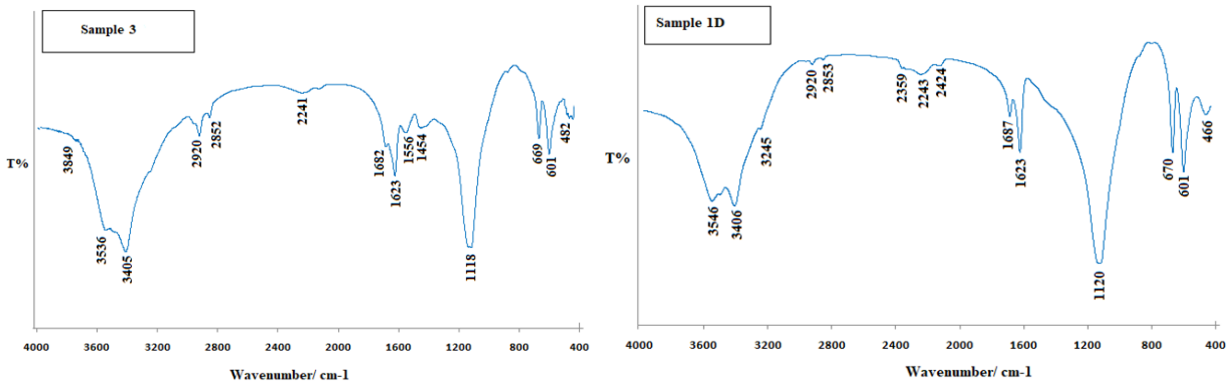

Figure 6. FTIR spectra of animal glue used in adhesion and reassembly of the mask (3) and stucco (1D).

3.5. DTA/DTG ANALYSIS

Fig. 7 shows the DTA/DTA curves obtained on the stucco sample (1E). The differential thermal curve (DTA) of the sample showed a peak at about (140^{o}C) relates to gypsum dehydration, while the peak detected at about (880^{o}C) is related to calcite decomposition (Fig. 7A) [21]. The DTG analysis showed a mass loss (18.897%) between 82 and 261^{o}C which reflects the dehydration of gypsum, while the mass loss (5.55%) between 790 and 1001^{o}C is due to the loss of CO_2 as a consequence of the decomposition of calcite ratio. The high loss ratio of gypsum dehydration when compared to the mass loss of calcite decomposition may reflect the high ratio of gypsum binder in the stucco of the mask, which confirms the results of XRD analysis (Figs. 7B and 7C) [22].

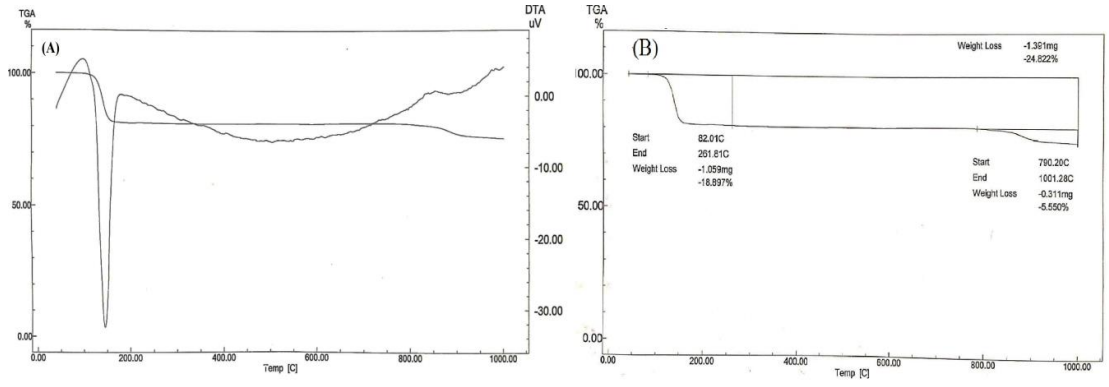

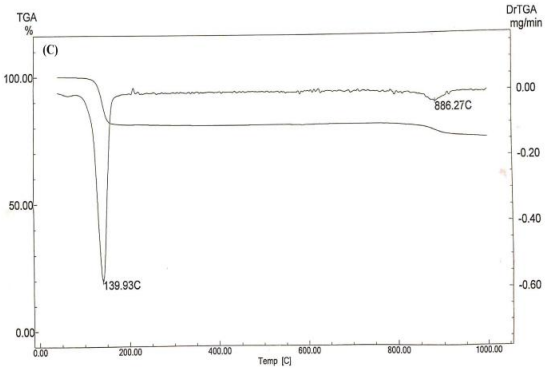

Figure 7. DTA/DTG curves of the mask stucco sample (1E).

2.6. MICRO-RAMAN ANALYSIS

Fig. 8 comprises the μ-Raman spectra on the studied pigment samples. The spectrum recorded on the red-orange pigment sample from edges of the chest area (sample 4R) reported a collection of bands at 221, 288, 408, 605 and 628 cm^{-1} which refer to the Fe−O bonds of ferrix oxide of hematite mineral (α-Fe_2O_3). Further, the bands reported at 670, 1020, and 1080 cm^{-1} are for Si−O−Si asymmetric stretching vibrations. These findings suggest that red ochre (hematite associated with clay minerals) most probably was used to decorate the stucco mask.

The Raman spectrum on a brown pigment sample from the chest area (sample 5B) shows a Si–O stretching band (ν_3 antisymmetric stretching) at 1001 cm^{-1} together with a small band at 1105 cm^{-1}. The bands at 418, 552 and 618 cm^{-1} are for hematite and the one at 662 cm^{-1} is probably for magnetite (Fe_3O_4), which explains, to some extent, the brownish appearance of the pigment.

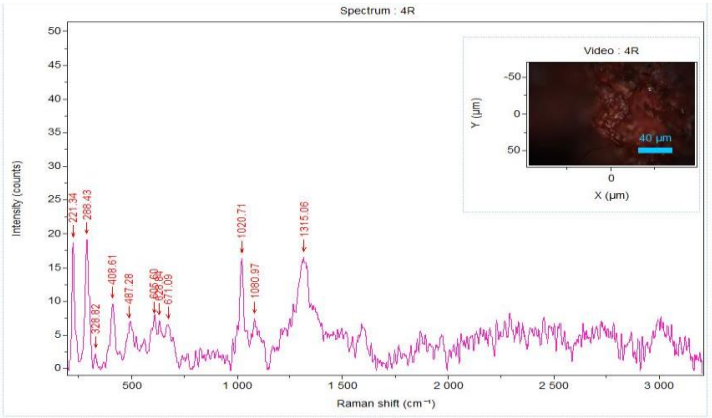

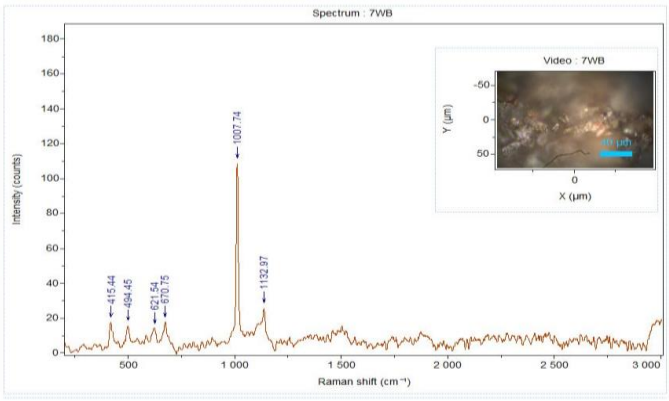

Figure 8. µ-Raman spectra of: red-orange pigment sample from edges of the chest area (4R), brown pigment sample from the chest area (5B), and brown and white grains from the face area (7WB).

The Raman spectrum on different brown and white grains from the face area (sample 7WB) showed sulfate symmetric stretching (ν_1) of gypsum appears at 1007, 670 and 621 cm^{-1}. While the band recorded at 1131 cm^{-1} is most probably for anhydrite. More, the bands at 415 and 494 cm^{-1} are for the E_g and A_{g1} vibrational modes assigned to hematite, respectively [20, 23, 24].

4. CONCLUSIONS

This study is an initial part of the conservation procedures designed for a Greco-Roman stucco mask (Reg. No. 229) which preserved in stores of the National Museum of Egyptian Civilization of Cairo, Egypt (NMEC). This archaeometric study helps in identifying the mineralogical composition of the stucco mask as the results revealed minerals of gypsum and calcite as the components of the mask. The pigments used to decorate the mask were of hematite for the red-orange color, mixture of hematite and magnetite for the brown color and mixture of gypsum and hematite for the white brown color. The used adhesive is animal glue and the deterioration aspects were mainly of anhydrite and halite salts. The iron nails, probably used in old intervention to the stucco mask, produced several corrosion products which caused a notable discoloration. Noteworthy when removing the halite salts from the studied mask to consider the recommendations concerning the removal of highly soluble salts from stucco artifacts. Finally, when designing the conservation strategy it is important to consider controlling the museum and store environment as a principal requirement.

Acknowledgment: *This study is a part of project entitled 'Developing Innovative Eco-Friendly Materials for Restoration Purposes of Archaeological Lime-based Mortars and Plasters' funded by the General Administration of Scientific Research of Cairo University.*

REFERENCES

[1] McCrimmon, M., *American Journal Archaeology*, **49**(1), 52, 1945.
[2] Darwish, S. S. A, *General Union Arab Journal*, **22**(2), 125, 2021.
[3] Svoboda, M., Cartwright, C.R., *Mummy Portraits Roman Egypt, Emerging Research from the APPEAR Project*, J. Paul Getty Trust, 159, 2020.

[4] Frederiksen, R., *Plaster Casts: Making, Collecting and Displaying from Classical Antiquity to the Present*, Eds. Frederiksen, R., Marchand, E., De Gruyter, Germany, 15, 2010.
[5] Vandenbeusch, M., O'Flynn, D., Moreno, B., *Journal Egyptian Archaeology*, **107(**1-2), 282, 2021.
[6] Bintintan, A., Gligor, M., Radulescu, C., Dulama, I.D., Olteanu, R.L., Stirbescu, R.M., Teodorescu, S., Bucurica I.A., *Analytical Letters*, **52**(15), 2348-2364, 2019.
[7] Bintintan, A., Gligor, M., Dulama, I.D., Radulescu, C., Stihi, C., Ion, R.M., Teodorescu, S., Stirbescu, R.M., Bucurica, I.A., Pehoiu, G., *Romanian Journal of Physics*, **64**(5-6), 903, 2019.
[8] Middendorf, B., *Natural Stone, Weathering Phenomena, Conservation, Strategies and Case Studies*, Geological Society, London, Special Publications, **205**, 173, 2002.
[9] https://geology.com/minerals/gypsum.shtml.
[10] *The Builders Standard Catalogue*, 10th Edition, The White Friars Press Ltd, London of Ton Bridge, England, Section 4, 1955, pvi.
[11] Kamel, A.M.A., Marie, H.A.H., Mahmoud, H.A., Ali, M.F, *Periodico di Mineralogia*, **83**(3), 318, 2014.
[12] Marie, H.A.H., *Geologic and Experimental Geochemical Studies on Some Anhydrite Deposits along the Gulf of Suez.* Ph.D. Thesis, Faculty of Science, Zagazig University, 1996.
[13] Mora, P., Mora, L., Philippot, P., *Conservation of Wall Painting*, ICCROM, 186, 1984.
[14] Hussein, A., Madkour, F., Afifi, H., *Egyptian Journal Archaeological Restoration Studies*, **8**(2), 114, 2018.
[15] Kamel A.M.A., *Scientific Culture*, **5**(2), 50, 2019.
[16] Kamel, A.M.A., El Ghanam, M.A., Khedr, M.S.A., *Acta Physica Polonica A*, **135**(3), 358, 2019.
[17] Kamel, A.M.A., Marie, H.A.H., et al, *Construction Building Materials*, **101**, 700, 2015.
[18] Derrick, M.R., Stulik D., Landry, J.M., *Infrared Spectroscopy in Conservation Science: Scientific Tools for Conservation*, the Getty conservation institute, J. Paul Getty Trust, 181, 195, 1999.
[19] Ali, M.F., Abd Elkawy, M.H., *Scientific Culture*, **7**(1), 45, 2021.
[20] Marey Mahmoud, H.H.M., *Heritage Science*, **2**, 18, 2014.
[21] Alvarez, J. I., Montoya, C., Navarro, I., Martin, A., *9th Inter. Cong. on Deter. and Cons. of Stone*, **2**, 878, 2000.
[22] Duran, A., Perez Maqueda, et al., *Journal Thermal Analysis Calorimetry*, **99**, 803, 2010.
[23] Hussein, A. M., Madkour, F. S., Afifi, H. M., Abdel Ghani, M., Abd Elfatah, M., *Vibrational Spectroscopy*, **106**, 1, 2020.
[24] Salama, K. K., Ali, M. F., El Sheikh, S., *Journal Science Arts*, **1**(46), 153, 2019.